Journal of Medical Systems (2019) 43: 291
https://doi.org/10.1007/s10916-019-1403-5

IMAGE & SIGNAL PROCESSING

A Novel Algorithm for Hyperspectral Image Denoising in Medical Application

Kirubanandasarathy Nageswaran[1] · Karthikeyan Nagarajan[2] · Ramasubramanian Bandiya[3]

Received: 3 April 2019 / Accepted: 25 June 2019 / Published online: 23 July 2019
© Springer Science+Business Media, LLC, part of Springer Nature 2019

Abstract
The one of the preprocessing step for hyperspectral imagery is noise reduction. The images are received by the detector and this can be degraded by several factors like atmospherical things and device noises which emit temperature noise, processing noise and explosion noise. There are several strategies are developed already to cut back the signal to noise magnitude relation of the hyperspectral image. However, the stationary noise of the many denoising ways developed cannot be applied on to the gauge boson noise. Thus, the each gauge boson and thermal noise square measure gift within the captured hyperspectral image (HSI). during this paper, we tend to projected a replacement denoising framework known as tensor-based filtering employing a PARAFAC tensor decomposition methodology for scale back each noise. The proposed technique is performs higher in removing noise as compared with different strategies like Multiple linear regression (MLR) algorithm and combined algorithm called multidimensional wavelet transforms with multiway wiener filter (MWPT-MWF) technique. The performance analysis of the new denoising framework has more efficient for reducing signal dependent (PN) and signal independent noise (TN) as compared with other conventional method. Hence this novel denoising approach would be more beneficial for detection of skin allergy and also this algorithm will be very useful for detection of retinal exudates and diagnosis of diabetes mellitus and retinopathy disease in medical application.

Keywords PARAFAC · Novel denoising technique · Hyperspectral image · Medical application

Introduction

The hyperspectral Image (HSI) would possibly stand a 3 dimensional (3D) statistics consolidated shape that speaks in accordance with in twain measurements, introductory two measurements speak in conformity with spatial information or moreover the measurement speaks in accordance with the spectral records regarding a scene. Figure 1 demonstrates companion quantity illustration regarding a hyperspectral facts shape. The capture data is received from Hyperspectral space-borne sensors in many slender spectral bands, rather than one wide spectral band. The determined image will give careful spectral data of the scene. The determined hyperspectral image (HSI) is degraded by totally different sources by system and setting. Therefore, the noise free estimation is to be needed; therefore this noise free estimation is represented as "denoising".

The obtained pictures from hyperspectral camera area unit degraded by several sources like region effects and instrumental noises. By providing coefficient of reflection, the atmospherical effects is also remunerated, however the sensor noise is consist of three noises which can be called as photon, thermal and quantization noise that results the spectral band will be corrupted by the way of different degrees. This corrupted spectral band is degrading the hyperspectral image analysis potency thus this is

This article is part of the Topical Collection on *Image & Signal Processing*

✉ Kirubanandasarathy Nageswaran
dr_nksarathy@syedengg.ac.in

Karthikeyan Nagarajan
nkarthikkeyan@gmail.com

Ramasubramanian Bandiya
ramabannada87@gmail.com

[1] Department of Electronics & Communication Engineering, Syed Ammal Engineering College, Ramanathapuram 623 502, India

[2] Department of Computer Science and Engineering, Syed Ammal Engineering College, Ramanathapuram 623 502, India

[3] Department of Computer Science and Engineering, Sarathy Sarojini Engineering College, Bangaluru, Karnataka, India

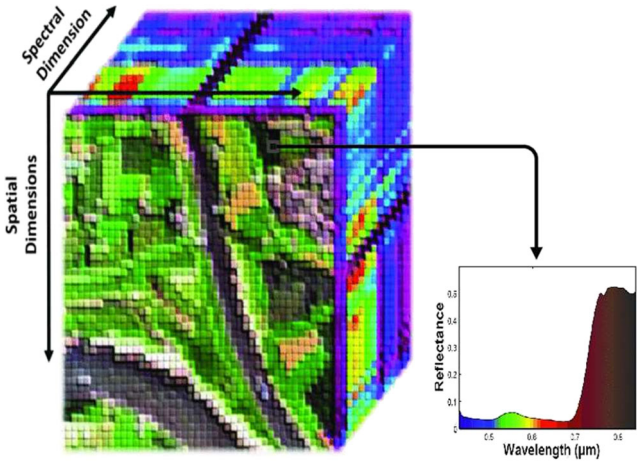

Fig. 1 The hyperspectral data cube with its reflectance pixel

often far from the information before to any extent further process. To improve the signal to noise quantitative relation (SNR) of hyperspectral image, HSI denoising is a concept about namely a preprocessing method among HSI analysis. For sensors utilized in hyperspectral imagination, there are two fundamental classifications over the random noise that are signal independent (TN) noise and signal dependent (PN) noise. [1, 2]. The charged coupled device (CCD) digicam resolution has been increased considerably, among order so much the photon noise has turn out to be as much dominant because the signal-independent digital noise of HSI statistics accumulated by using new-generation hyperspectral sensors [1–6]. The commonly used signal dependent and signal independent noise model have been conjointly proposed recently, anywhere the hyper-spectral noise parameter estimation algorithmic rule used to be projected. After standard Gaussian measurement for noise whitened in every band, the hyper-spectral noise parameter estimation uses the assumption for removing both noises. Here we proposed tensor-based technique for removal of above said noises (www.mdpi.com/2072-4292/10/9/1330/htm).

The two classifications of random noise model in HSIs have spectral and spatial parameters including with white noise [6–10], and the white Noise is constant with spatial parameter but this is varied in the spectral parameter [11, 12]. This is entirely sensible procedure during the overwhelming of the thermal noise [4]. In any case, these two noise models must be appropriate during the consideration of signal dependent noise. Based on scatter plot estimation of signal dependent photon noise parameters was proposed by Aiazzi et al. in [13, 14]. Regardless, the signal dependent noise is not appropriate in hyperspectral image which is discussed by B. Aiazzi et al. Argenti et al. was presented most precise common signal dependent noise model for digital image [15, 16] and also measured the noise value in wavelet domain using Linear Minimum Mean Square Error (LMMSE) [1] (www.mdpi.com/2072-4292/10/9/1330/htm).

In this paper, we proposed another denoising system called tensor-based algorithm utilizing a PARAFAC rank decomposition technique. The proposed denoising framework performs better in removing noise as compared with other two methods such as Multiple Linear Regression (MLR) method [1] and combined both multidimensional wavelet packet transform and multi-way Wiener filter method (MWPT-MWF) method. Thus, the proposed method has confirmed advantages as compared to other denoising method.

Related works

Multiple linear regression (MLR) technique

Multiple linear regression (MLR) is a measurable system which utilizes a few illustrative factors to anticipate the result of a response variable. The HYNE means hyperspectral noise estimation method. The HYNE method is based on the Multiple linear Regression (MLR). MLR is used as common basis for three analysis methods used in the unscramble such as Multiple Linear Regression, Analysis of Effects and Response Surface Analysis (www.investopedia.com).

The Multiple linear regression models for n clarifications can be represented by following expression,

$$m_k = A_0 + A_1 x_{k1} + A_2 x_{k2} + \ldots\ldots + A_p x_{kp} + R_e \quad (1)$$

where $k = 1,2, \ldots, n$ and Re is random error prediction.

The value $A_0, A_1, A_2 \ldots Ap$ are least squares estimates which is calculated by using arithmetically derivative program. As many variables can be blanketed within the regression model in which every unbiased variable is differentiated with a range of $1, 2, 3, 4 \ldots p$. The couple of regression model lets in an analyst to predict the final results based on facts provided on more than one explanatory variable (www.investopedia.com). Nonetheless, the model isn't always usually perfectly accurate as every information point can vary slightly from the final results expected through the model. The residual value R, that's the difference among the real outcome and the anticipated outcome, is included inside the model to account for such moderate variations (www.investopedia.com).

The co-efficient of determination, R^2, could be applied math metric that's accustomed live what quantity of the variation in outcome will be explained by the variation within the freelance variables. R^2 forever will increase as additional predictors are superimposed to the MLR model even if the predictors might not associated with the result variable (www.investopedia.com). Therefore, R^2 by itself, cannot be accustomed determine that predictors ought to be enclosed in an exceedingly model and that ought to be excluded. R^2 will solely be between zero and one, wherever zero indicates that the result cannot be predicted by any of the freelance variables and one indicates that the result

will be predicted while not error from the freelance variables (www.investopedia.com).

To shape the Maximum likelihood rule, the joint probability density function (PDF) of the brightened noise value is utilized. In any case, the values of SNR were thought to be identified in the Maximum Likelihood model that was not valid in viable circumstances. Henceforth, the multiple linear regression hypothesis built methodology has abused to calculate them. Be that as it may, MLR is a one sided estimator when figures the noise value by limiting the Least Square Error (LSE), because noise isn't white. Therefore, the appraisal of multiple linear regressions has not precise in hyper-spectral noise parameter estimation, prompting the incorrectness of the last parameter calculation. During this study, the significance of another noise filtering structure in hyperspectral image is also examined for limiting all signal dependent explosion noise and signal independent temperature noise [17] (www.mdpi.com/2072-4292/10/9/1330/htm). The noise deviation is caught with the signal when taking into account, to minimizing the noises in hyperspectral image a novel denoising algorithm is proposed (www.mdpi.com/2072-4292/10/9/1330/htm).

A hyperspectral image is locally mutually handled in the spatial and spectral measurements inside a multi segment scanning window (MSW), as little as spatial-spectral pixels. Each MSW is viewed as an added substance blend of spectrally corresponded fractal Brownian movement - tests and random samples [17, 22]. Principal components analysis (PCA) is viable at compacting data in multivariate informational collections by figuring symmetrical projections that amplify the measure of information variance. Unpardonably, data content in hyperspectral pictures does not generally concur with such projections [18].

The multiple linear regression hypothesis assesses the signal by abusing the solid spectral relationship of the strong and weak signal versus random noise band relationship in the hyperspectral image. We imagine that the measurement of signal in horizontal vector $\widehat{Z}_{k_3}^T$. The subordinate value k_3 is undeviating factor of the blaring information. The horizontal vector $v_{j_3}^T(j_3 = 1, ..., k_3{-}1, k_3 + 1, ..., k_3)$ in alternate $k_3 - 1$ bands (www.mdpi.com/2072-4292/10/9/1330/htm):

$$X_{k_3} = \Theta_{k_3} w_{k_{3'}} \tag{2}$$

The value $\Theta_{k3} = [i_1, ..., i_{i3}{-}1, i_{k_3} + 1, ..., i_{k_3}]$ and $w_{k_3} \in G^{(k_3-1)}$ are the combined weight vector. By decreasing linear spectral estimation, resultant the maximum weight vector can be measured by equation [1]:

$$\widehat{w}_{k_3} = \arg\min_{w_{k_3}} \left\| r_{k_3} - \widehat{x}_{k_3} \right\|^2 \tag{3}$$

The linear spectral estimation issue result is recognized and can be denoted as:

$$\widehat{w}_{k_3} = \left(\Theta_{k_3}^T \Theta_{k_3}\right)^{-1} . \Theta_{k_3}^T r_{k_{3'}} \tag{4}$$

Finally the corresponding signal $\widehat{X}_{k_3}$ and noise $\widehat{n}_{k_3}$ are estimated and represented by:

$$\widehat{X}_{k_3} = \Theta_{k_3} \widehat{w}_{k_{3'}} \tag{5}$$

$$\widehat{n}_{k_3} = r_{k_3} - \widehat{X}_{k_{3'}} \tag{6}$$

The signal and noise were estimated from above Eqs. (5) & (6), then by optimizing likelihood function, the noise variances δ_{u,k_3}^2 and δ_{t,k_3}^2 can be assessed by the following equation [1, 4]:

$$\left\{ \delta_{u,k_3}^2, \delta_{t,k_3}^2 \right\} = \underset{\substack{\sigma_{u,k_3} \rangle n \\ \sigma_{t,k_3} \rangle n}}{brq\, opt}\ \lg\left(\sigma_{u,k_3}, \sigma_{t,k_3}\right) \tag{7}$$

Includes

$$\begin{aligned} \lg\left(\sigma_{u,k_3}, \sigma_{t,k_3}\right) &= -\frac{N}{2} \lg(2\pi) \\ &= -\frac{1}{2} \sum_{i_{k1}=1}^{K_1} \sum_{k_2=1}^{K_2} \lg\left[\sigma_{u,k_3}^2 . X_{k_1 k_2 k_3} + \sigma_{t,k_3}^2\right] \\ &= -\frac{1}{2} \sum_{k_1=1}^{K_1} \sum_{k_2=1}^{K_2} \frac{n_{k1 k_2 k_3}^2}{\sigma_{u,k_3}^2 . X_{k_1 k_2 k_3} + \sigma_{t,k_3}^2} \end{aligned} \tag{8}$$

Meanwhile signal and noise are unidentified factor in a genuine situation, The signal can be changed and calculated by the eqs. (5) and the noise can be changed and calculated by the eqs. (6) (www.mdpi.com/2072-4292/10/9/1330/htm). The MLR method can be computed by following Fig. 2.

Multidimensional wavelet packet transform and multi-way wiener filter

Multidimensional Wavelet Packet Transform (MWPT) can be calculated by executing one dimensional wavelet transform in each and every approach [19, 21]. Thus, the wavelet transform coefficient factor F_1^R is expressed as,

$$F_1^R = P \times \widehat{W}_1^{Z_1} \times \widehat{W}_2^{Z_2} \times \widehat{W}_3^{Z_3} \tag{9}$$

The above eq. (9) can be rewritten as

$$P = F_1^R \times \left(\widehat{W}_1^{Z_1}\right)^T \times \left(\widehat{W}_2^{Z_2}\right)^T \times \left(\widehat{W}_3^{Z_3}\right)^T \tag{10}$$

Since $Z = [Z_1, Z_2, Z_3]^T$, and $Z_1, Z_2, Z_3 \geq 0$. In particular, when $Z_1, Z_2, Z_3 > 0$, The Multidimensional Wavelet Packet Transform specifies the three dimensional wavelet transform. The value $\widehat{W}_k^{Z_k}$ is the Z_k level of wavelet transform to the kth P factor. $F_{1,n}^P$ can be denoted as the coefficient of F_1^P, here, the

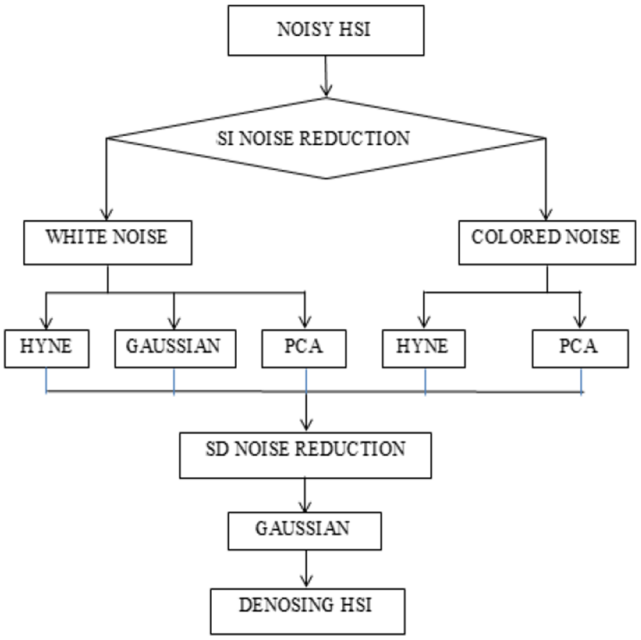

Fig. 2 Flow Chart of HYNE algorithm

factor $n = [n1, n2, n3]^T$ is the key vector, and $0 \leq nk \leq 2zk - 1$, since the factor k is considered as 1, 2, 3. The individual components of $F^P_{1,n}$ is calculated as (www.mdpi.com/2072-4292/10/9/1330/htm):

$$F^P_{1,n}(m_1, m_2, m_3) \triangleq F^P_1(M_1(m_1), M_2(m_2), M_3(m_3)) \tag{11}$$

where

$$\left\{ M_n = \left[\frac{j_n Z_n}{2^Z}, \ldots \frac{(j_n+1)Z_n}{2^Z} - 1 \right]^T, n = 1, 2, 3 \right\}$$

$$m_n \in \left\{ 1, \ldots, \frac{R_n}{2^Z} \right\}, n = 1, 2, 3. \tag{12}$$

The notation $F^P_{1,n}$ *(m1,m2, m3)* is the components of $F^P_{1,n}$ at point *(m1, m2, m3)*. We can identify the mode n 'frequency' is *jn* which is obtained by wavelet transform property. Therefore, *j* is considered as coefficient frequency index $F^P_{1,n}$ [23].

The algorithm is useful based on the multiway wiener filter rule to apply in HSI. The calculation of the signal topological space or grade in every method requires the filter for minimizing the littlest eigenvalues [20] (www.mdpi.com/2072-4292/10/9/1330/htm). A few unstrengthen signal may well be cutoff during the process. Hence, the signal to noise ratio is a crucial issue manipulating the grade. Once the signal to noise ratio is increases, the grade will be greater (www.mdpi.com/2072-4292/10/9/1330/htm), therefore, many signals are well-kept surrounded by the cleaning method. On other hand, a lot of signals are missing. The noise facility in every element $F^P_{1,n}$ during white noise is same, but the signal focuses within the minimal frequency element. The signal to noise ratio is totally different which mention in the numerous parts. A lot of signal will be conserved in every element during multiway wiener filter algorithm is functioned. Carried out the Multidimensional Wavelet Packet Transform to the factor *E*, *P* and *Q* in below equation [1],

$$E = P + Q \tag{13}$$

The derived equation as follows:

$$\begin{aligned} & E \times \widehat{W}_1^{Z_1} \times \widehat{W}_2^{Z_2} \times \widehat{W}_3^{Z_3} \\ & = (P + Q) \times \widehat{W}_1^{Z_1} \times \widehat{W}_2^{Z_2} \times \widehat{W}_3^{Z_3} \\ & = P \times \widehat{W}_1^{Z_1} \times \widehat{W}_2^{Z_2} \times \widehat{W}_3^{Z_3} + Q \times \widehat{W}_1^{Z_1} \times \widehat{W}_2^{Z_2} \times \widehat{W}_3^{Z_3} \end{aligned} \tag{14}$$

The every coefficient part is described as

$$F^E_1 = E \times \widehat{W}_1^{Z_1} \times \widehat{W}_2^{Z_2} \times \widehat{W}_3^{Z_3} \tag{15}$$

$$F^P_1 = P \times \widehat{W}_1^{Z_1} \times \widehat{W}_2^{Z_2} \times \widehat{W}_3^{Z_3} \tag{16}$$

$$F^Q_1 = Q \times \widehat{W}_1^{Z_1} \times \widehat{W}_2^{Z_2} \times \widehat{W}_3^{Z_3} \tag{17}$$

The coefficient factor$\hat{Q}$

$$\hat{F}^Q_1 = \hat{Q} \times \widehat{W}_1^{Z_1} \times \widehat{W}_2^{Z_2} \times \widehat{W}_3^{Z_3} \tag{18}$$

From the above eq. (11), we can find out each and every coefficient elements of the frequency $F^E_{1,n}$, $F^P_{1,n}$ and $F^Q_{1,n}$ from F^E_1, F^P_1 and F^Q_1 respectively [1] and then it can be written as:

$$F^E_{1,n} = F^P_{1,n} + F^Q_{1,n} \tag{19}$$

The subsequent expression can be derived based on Parseval's theorem (www.mdpi.com/2072-4292/10/9/1330/htm):

$$\left\| Q - \hat{Q} \right\|^2 = \left\| F^Q_1 - \hat{F}^Q_1 \right\|^2 = \sum_n \left\| F^Q_{1,n} - \hat{F}^Q_{1,n} \right\|^2 \tag{20}$$

The above expression represents that reducing the mean square error of Q and $\hat{Q}$.Resultants, this appreciate to reducing mean square error between $F^Q_{1,n}$ & $\hat{F}^Q_{1,n}$. The $\hat{F}^Q_{1,n}$ can be estimated through Tucker3 based decomposition of$F^E_{1,n}$. Thus,

$$\hat{F}^Q_{1,n} = F^E_{1,n} \times L_{1,n} \times L_{2,n} \times L_{3,n} \tag{21}$$

then $L_{1,n}$, $L_{2,n}$, $L_{3,n}$ represents the multi-way Wiener filter 'n' method [19]. Applying inverse multidimensional wavelet packet Transform, we calculate $\hat{Q}$ That is given by

$$\hat{Q} = \hat{F}_1^Q \times \left(\widehat{W}_1^{Z_1}\right)^T \times \left(\widehat{W}_2^{Z_2}\right)^T \times \left(\widehat{W}_3^{Z_3}\right)^T \quad (22)$$

The flow chart of MWPT-MWF algorithm is shown in Fig. 3.

Proposed work

The Parallel factor analysis (PARAFAC) may be a best decomposition methodology which is concept wise related to bilinear orthogonal transformation called Principle Component Analysis (PCA). But the Tucker3 decomposition is derived from higher order generalization of PCA. A decomposition of the information is formed into triplets or tri-linear parts, however, rather than the single score vector and the single loading vector as in additive bilinear orthogonal transformation and the every element has single score vector and multiple loading vectors. The specific advantage of the proposed model is individualism of the result (www.models.kvl.dk). The additive strategies is widely branded drawback of motion liberty. The main reason has encouraged plenty of various ways for getting additional explicable systems as than principle component analysis [24]. In this paper, we have a tendency to propose a denoising technique referred to as PARAFAC decomposition methodology based on tensor filtering ()www.mdpi.com/2072-4292/10/9/1330/htm.

The prime objectives are to get the clean signal estimation $\hat{Q}$ this is very important for derive the noise discrepancy.

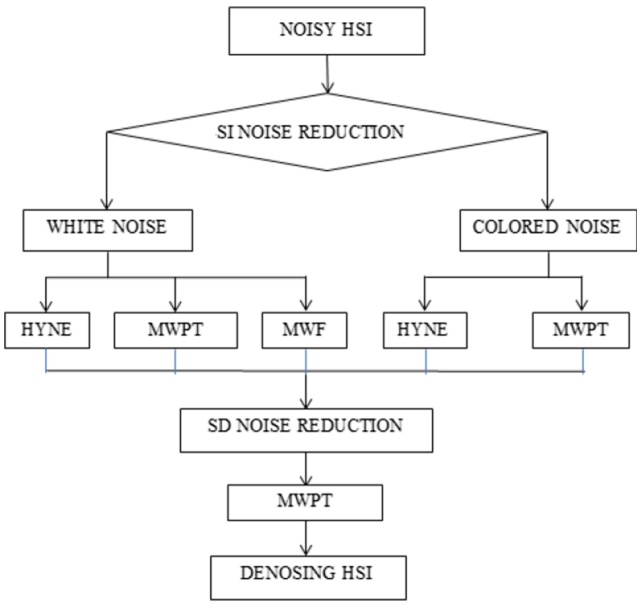

Fig. 3 Flow Chart of MWPT-MWF algorithm

However, meanwhile the noise is present in signal; the noise discrepancy of R is totally differing from others. This is related to the signal p_{i1i2i3} (www.mdpi.com/2072-4292/10/9/1330/htm). The noise q_{i1i2i3} could be an addition of Gaussian distribution variables x_{i1i2i3} and y_{i1i2i3}. Hence, $q_{i1i2i3} = \sqrt{p_{i1i2i3}}.x_{i1i2i3} + y_{i1i2i3}$ could be a random variable which obtained by Gaussian distribution. Therefore,

$$q_{i1i2i3} \approx M\left(0, \sigma^2_{q_{i1i2i3}}\right) \quad (23)$$

Here, M is the general distribution; the noise discrepancy is represented as $\sigma^2_{q_{i1i2i3}}$. This could be derived as,

$$\begin{aligned}\sigma^2_{q_{i1i2i3}} &= E\left[\left(\sqrt{p_{i1i2i3}}.x_{i1i2i3} + y_{i1i2i3}\right)^2 | q_{i1i2i3}\right] \\ &= p_{i1i2i3}.\sigma^2_{x,i3} + \sigma^2_{y,i3}\end{aligned} \quad (24)$$

The noise discrepancy calculation $\widehat{\sigma}^2_{qi1i2i3}$ wants the accurate signal calculation $\hat{p}^2_{q_{i1i2i3}}$. Therefore, the problems among signal and noise calculation are inter correlated. Based on multiple linear regression rules, the signal calculation created and then the noise factors are calculable by using it. By reducing least mean square error, the signal is estimated. Nevertheless, the signal and noise must be arithmetically freelance when the least mean square error calculator needs, that is not glad within the signal dependent explosion noise scenario (www.mdpi.com/2072-4292/10/9/1330/htm). Thus, the signal and also noise calculation aren't accurate, that generates the factor calculation outcome unpredictable similarly. Meanwhile we must have single stage for calculating the signal. Due to the inexact calculation of noise factor which leads to decrease the noise factor calculation efficiency [22].

From Eq. (24), the noise discrepancy $\sigma^2_{q_{i1i2i3}}$ is reliant on signal $p^2_{q_{i1i2i3}}$. To remove this connection, we have to whiten the noise (www.mdpi.com/2072-4292/10/9/1330/htm):

$$\underline{p}_{i1i2i3} = \frac{p_{i1i2i3}}{\sigma_{q_{i1i2i3}}} \approx M(0,1) \quad (25)$$

Here, we have differentiate the whiten information and the unique information by putting the underlined. We must care about the noise $\underline{p}_{i1i2i3}$ later on the blanching task that it is free from the whitened signal.

In this work, our proposed denoising technique referred to as PARAFAC decomposition methodology based on tensor filtering have produces the foremost correct signal calculation $\hat{\underline{p}}_{i1i2i3}$. Additionally, the well-known HYNPE algorithmic program allows getting the ML estimates of $\widehat{\sigma}^2_{x,i3}$ & $\widehat{\sigma}^2_{y,i3}$. During this paper, we elect to mix these 2 ways to urge a lot of correct noise discrepancy calculation for N. This is estimated as,

$$\widehat{\sigma}^2_{q_{i1i2i3}} = \hat{p}_{i1i2i3}.\widehat{\sigma}^2_{x,i3} + \widehat{\sigma}^2_{y,i3} \tag{26}$$

After attaining noise discrepancy of E, the brightened noise is written as:

$$\underline{e}_{i1i2i3} = \underline{p}_{i1i2i3} + \underline{q}_{i1i2i3} = \frac{\underline{p}_{i1i2i3}}{\widehat{\sigma}_{\underline{q}_{i1i2i3}}} + \frac{\underline{q}_{i1i2i3}}{\widehat{\sigma}_{\underline{q}_{i1i2i3}}} \tag{27}$$

Then the brightened HSIs is represented as,

$$\underline{E} = \underline{P} + \underline{Q} \tag{28}$$

Consistently with the hyperspectral image progress achieved, we have to end up PWP hoop; we have to find out end measure (www.mdpi.com/2072-4292/10/9/1330/htm). Finally, we can derive the foundation of Root Mean square Error (RSME) value. The before and after estimation of the signal can be written as,

$$RSME_P = \frac{\left\|\hat{P} - \tilde{P}\right\|^2}{I_1 I_2 I_3 \left\|\hat{P}\right\|^2} \tag{29}$$

From the above eq. (29), the before estimation is denoted as $\tilde{X}$ and the after estimation is denoted $\widehat{X}$. Generally the $RMSE_P$ value is stable during higher iteration. Therefore, we could find out the $RMSE_P$ relative error as end up criterion, we takes two adjacent iterations for the same. The relative error can be expressed as.

$$e = \frac{|RSME_P - RSME_P^0|}{RSME_P^0} \tag{30}$$

From the above expression, the final iteration is $RSME_X^0$. The conditional loop is end up when value of $e \leq$ value of ε. The Fig. 4 shows flow chart of proposed PARAFAC algorithm.

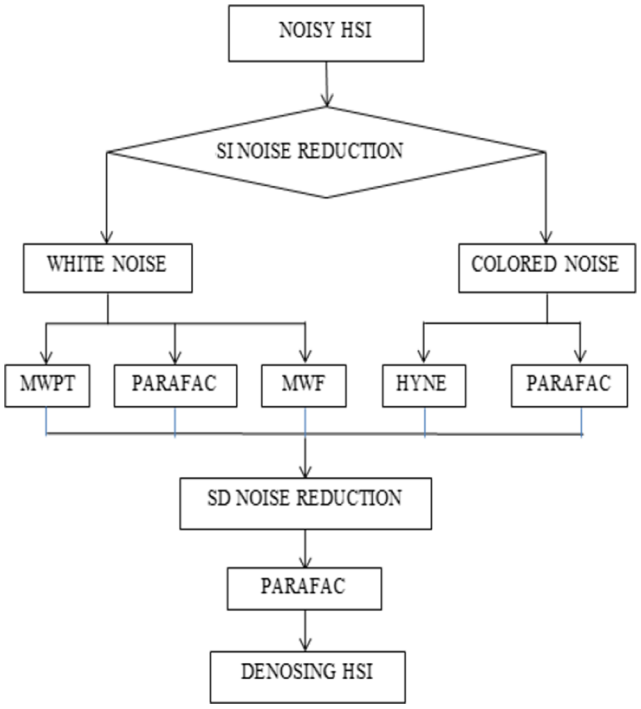

Fig. 4 Flow Chart of proposed PARAFAC algorithm

Experimental results and discussion

In the section, we have experimented various denoising methods that are frequently utilized to minimizing noise in hyperspectral images. The combined algorithm called multidimensional wavelet transforms with multiway wiener filter (MWPT-MWF) technique and multiple linear regression (MLR) technique were conventional method for denoising the hyperspectral image (www.mdpi.com/2072-4292/10/9/1330/htm). Hence, a new PARAFAC technique is proposed instead of these conventional algorithms. The performance of various denoising technique such as MWPT-MWF and MLR and the proposed PARAFAC method were carried out and their performance were analyzed with respect to means noise discrepancy. Here we have been setting the error value as 10^{-3} for all comparative methods. Figure 5a shows the color combinations of P and Fig. 5b shows color combination of E.

The Root Mean Square Error can be derived for both noise discrepancy of signal dependent (Photon Noise - PN) and signal independent (Temperature Noise - TN) noise as follows (www.mdpi.com/2072-4292/10/9/1330/htm),

$$RSME_{PN} = \frac{1}{I_3}\sum_{i3=1}^{I_3}\left(\frac{\widehat{\sigma}^2_{x,i3} - \sigma^2_{x,i3}}{\sigma^2_{x,i3}}\right)^2 \tag{31}$$

$$RSME_{TN} = \frac{1}{I_3}\sum_{i3=1}^{I_3}\left(\frac{\widehat{\sigma}^2_{y,i3} - \sigma^2_{y,i3}}{\sigma^2_{y,i3}}\right)^2 \tag{32}$$

From above equations, we can obtain low values for $RMSE_{PN}$ and $RMSE_{TN}$ which denote good estimation accuracy. The Comparative performance analyses for all algorithms have been done. The optimal iteration period is taken as 10 for evaluating the root mean square error for both noises [1]. Figure 6 shows mean value of noise discrepancy with band 20 dB. Figure 7 shows the output graph for $RMSE_{PN}$ versus iteration periods for different signal to noise value and Fig. 8 shows the output graph

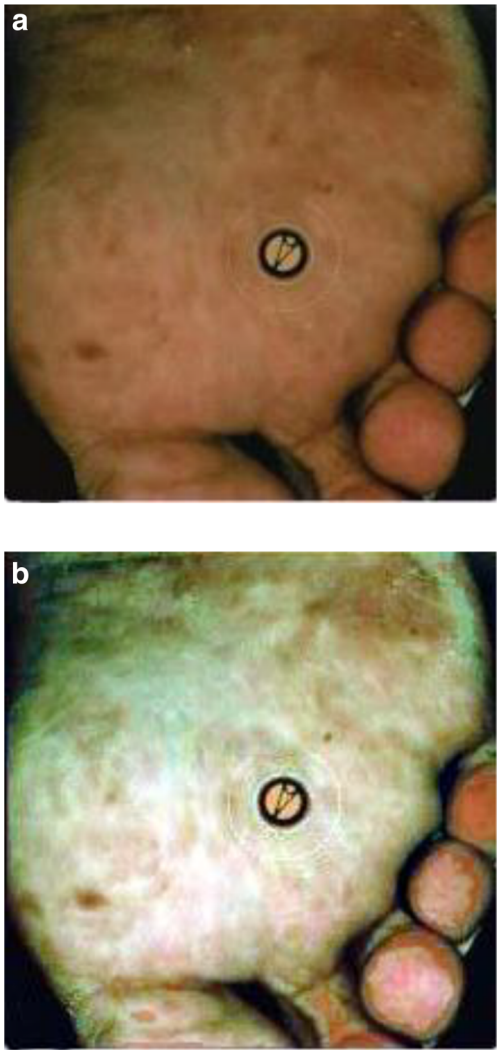

Fig. 5 **a** Color combination of *P*. **b** Color combination of *E*

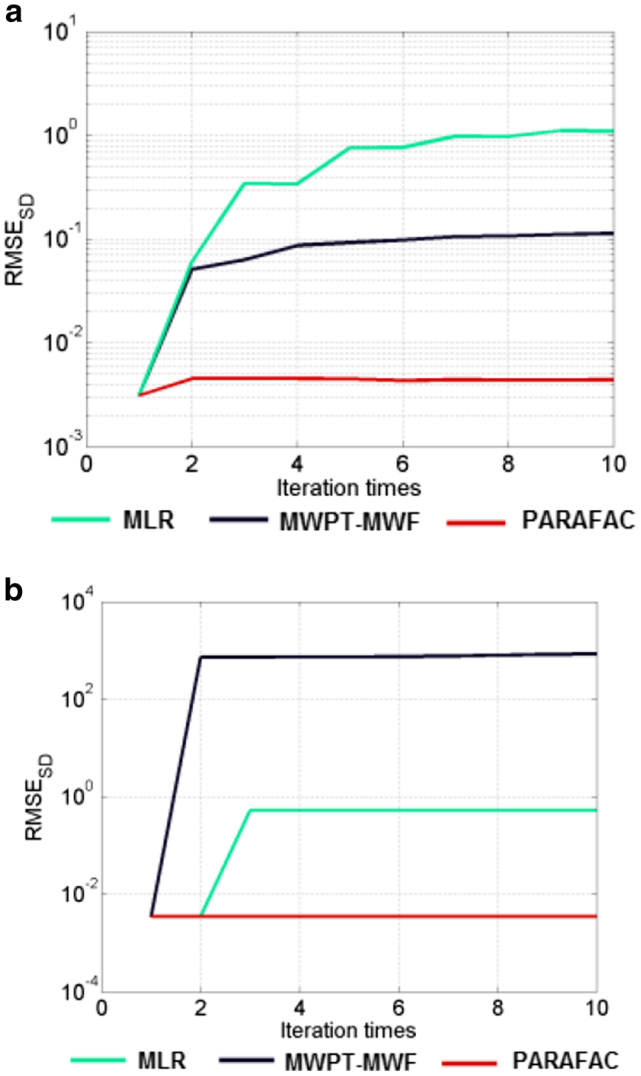

Fig. 7 **a** The output graph for $RMSE_{PN}$ vs iteration periods at 20 dB. **b** The output graph for $RMSE_{PN}$ vs iteration periods at 40 dB

of $RMSE_{TN}$ versus iteration periods for different signal to noise value. From Figs. 7a and 8a, we can observe that, when SNR_{INPUT} is 20 dB, the combined algorithm

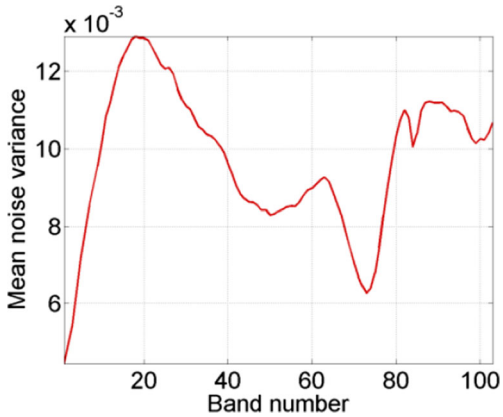

Fig. 6 Means value of noise discrepancy with band 20 dB

(Multidimensional wavelet packet transform with multiway wiener filter) is well performed than multiple linear regression algorithm (MLR) for both noise estimation (www.mdpi.com/2072-4292/10/9/1330/htm).

However, when SNR_{INPUT} is 40 dB, MLR is better than MWPT-MWF. But the both Figs. 7 and 8, the anticipated PARAFAC strategy could increase the calculation execution essentially in venture with the base $RMSE_{PN}$ and $RMSE_{TN}$ it gets. In addition, $RMSE_{PN}$ and $RMSE_{TN}$ region bigger than the underlying blunder in multiple linear regression and combined algorithm (Multidimensional wavelet packet transform with multiway wiener filter), though $RMSE_{PN}$ and $RMSE_{TN}$ are well unnatural in PARAFAC decay approach.

To naturally exhibit the noise brightening effects, Fig. 9 demonstrates the mean value of noise discrepancy of band at 20 dB later on the noise brightening task. It is clear from the Fig. 9 that proposed PARAFAC mean value of the noise discrepancy is

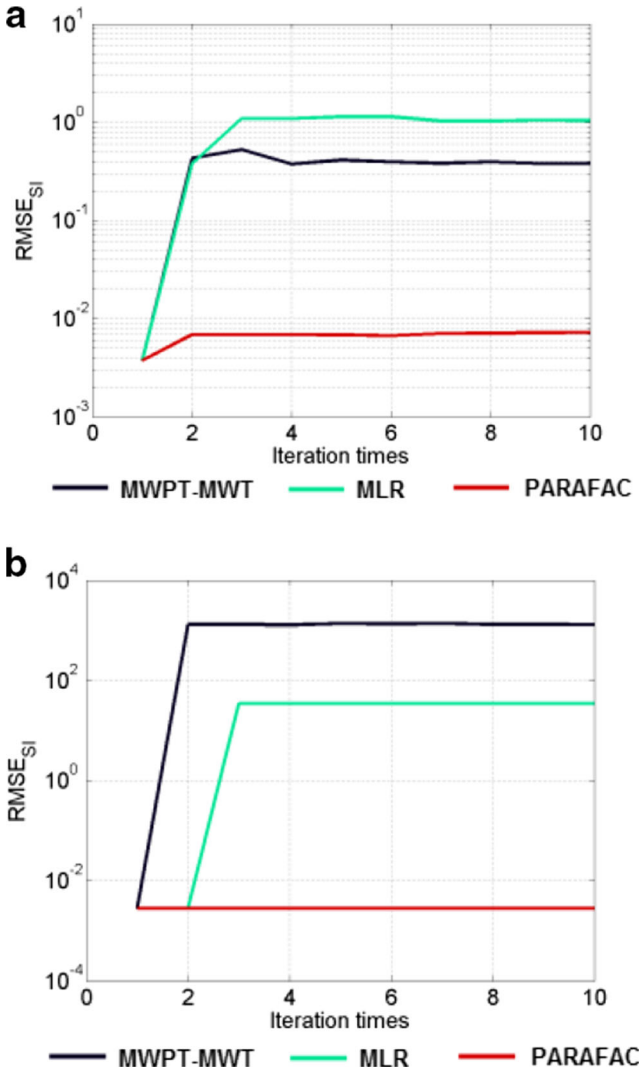

Fig. 8 **a** The output graph for $RMSE_{TN}$ vs iteration periods at 20 dB. **b** The output graph for $RMSE_{TN}$ vs iteration periods at 40 dB

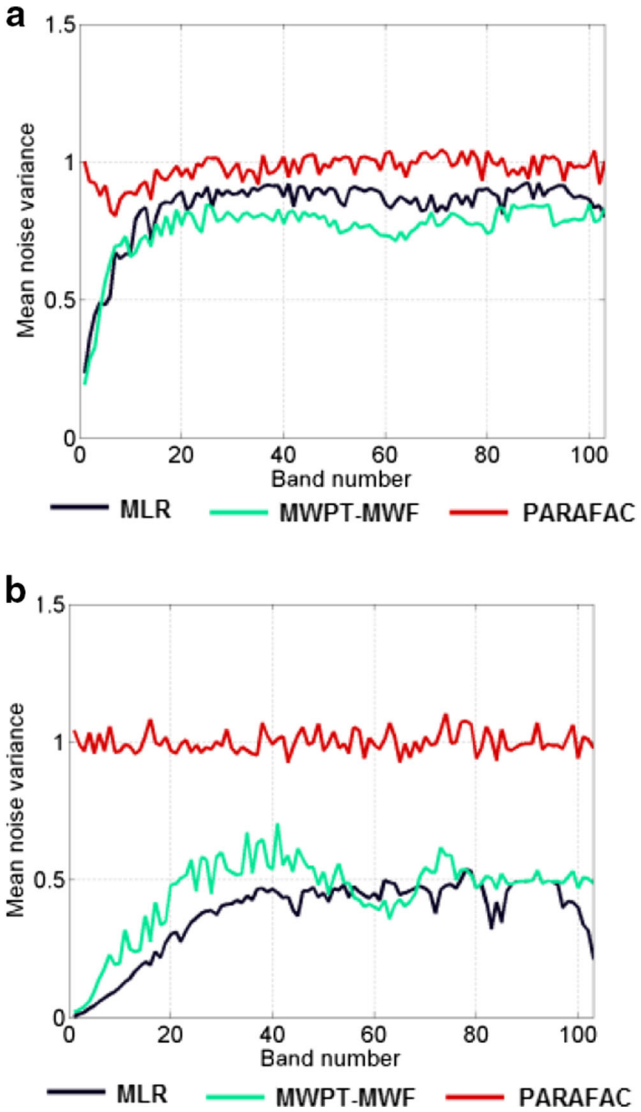

Fig. 9 **a** The output graph for Mean value of noise discrepancy vs band at 20 dB. **b** The output graph for Mean value of noise discrepancy vs band at 40 dB

unity (as 1). This is consistent concerning the band number. But the other conventional methods have generated not acceptable mean value of noise discrepancy (www.mdpi.com/2072-4292/10/9/1330/htm). From Fig. 8a, we observed that the lower band mean value of noise discrepancy is same as like in Fig. 6 but here the lower band noise (1 dB – 20 dB) is not all around brightened. Then again, the noise discrepancy values in higher bands (20 dB to 100 dB) are generally steady and the mean value of the noise discrepancy is not steady. From Fig. 8a, we could observed that the noise brightening outcomes of the conventional technique are more terrible than the Fig. 8 b. Subsequently, the proposed PARAFAC technique brightening results is presented in Fig. 9a and b.

The typical possibility graph has been generally utilized to determine regardless of whether set of information has roughly regularly circulated, this implies the qualities in the set of information has a same noise discrepancy (www.mdpi.com/2072-4292/10/9/1330/htm). Figure 10a presents a typical possibility graph during pre-brightening. From the Fig. 10a, we could clearly known that pre brightening of noise is not ordinarily circulated. Subsequent to brightening has taken by multiple linear regression technique as shown in the Fig. 10b and c by combined multidimensional wavelet pocket transform with multiway wiener filter, it can be seen that there is few qualities not all around brightened, it quiet continues the interval period [−5, 0] (www.mdpi.com/2072-4292/10/9/1330/htm). But the noise esteems in the wake of brightening by proposed PARAFAC structure has a straightforward line as shown in Fig. 10d. Thus the PARAFAC algorithm is considering as typically circulated.

In connection with above, Fig. 11a presents a typical possibility graph during pre-brightening. From the Fig. 11 a, we could clearly know that pre brightening of noise is not ordinarily circulated. Subsequent to brightening has taken by multiple linear

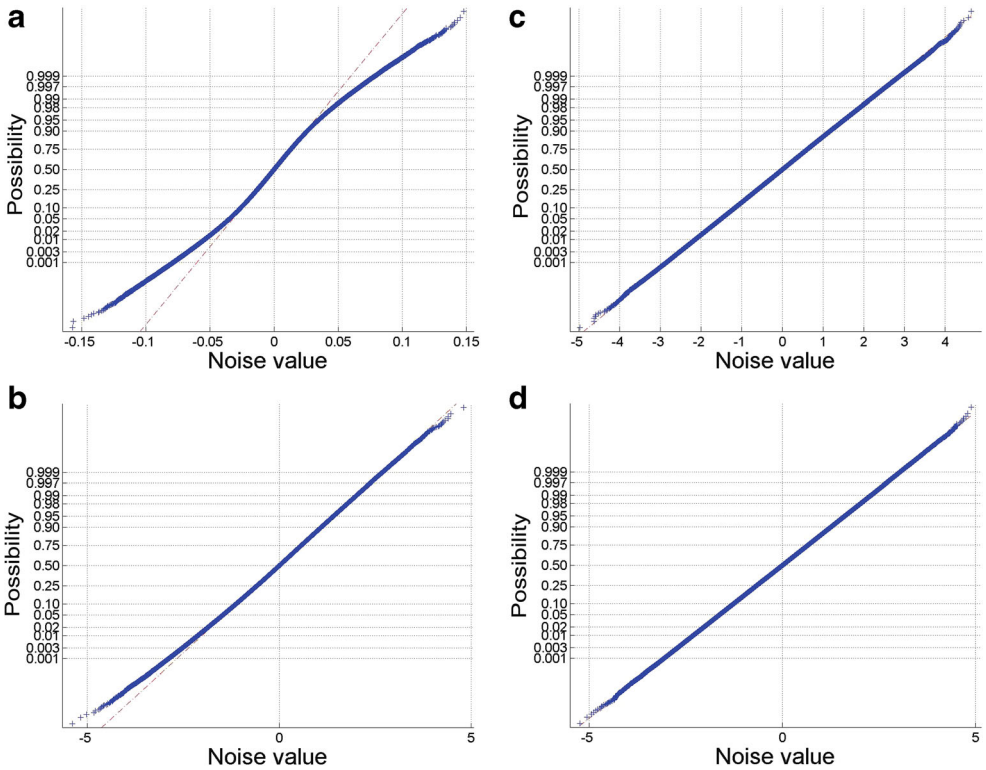

Fig. 10 **a** Possibility graph with noise at 20 dB. (Pre-brightening). **b** Possibility graph with noise at 20 dB (Using MLR). **c** Possibility graph with noise at 20 dB (Using MWPT-MWF). **d** Possibility graph with noise at 20 dB (Using PARAFAC)

regression technique as shown in the Fig. 11b and c by combined multidimensional wavelet pocket transform with multiway wiener filter, it can be seen that there is few qualities not all around brightened, it quiet continues the interval period [−5, 0] (www.mdpi.com/2072-4292/10/9/1330/htm). But the noise esteems in the wake of brightening by proposed PARAFAC structure has a straightforward line as shown in Fig. 11d. Thus the PARAFAC algorithm is considering as typically circulated. The outcomes from the Figs. 10 and 11 approve by the proposed PARAFAC algorithm has better performance in both noise band value (at 20 dB and 40 dB).

We demonstrate a few outcomes about the denoising execution. Figure 12a, b and c shows the noise expelled from hyperspectral image using Multiple Linear Regression, combined algorithm called Multidimensional Wavelet Packet Transform with Multiway Wiener Filter and PARAFAC algorithms in band 10 at 20 dB. We could identify from the real image in the Fig. 5a, the expelled noises are the signal dependent explosion noise by contrasting checking with the Fig. 12. From the Fig. 12, it was observed that the proposed PARAFAC structure has better performance in evacuating the signal dependent explosion noises (PN) in hyperspectral images.

Also, we have surveyed the denoising execution of different strategies by breaking down the basis SNR_{OUTPUT}. Figure 13a and b shows the advancement of the SNR_{OUTPUT} in different noisy situations. Clearly the SNR_{OUTPUT} produced by PARAFAC achieves a higher stable an incentive after a few cycles. On the other hand, the SNR_{OUTPUT} of Multiple Linear Regression and Combined algorithm of Multidimensional Wavelet Packet Transform with Multiway Wiener Filter have generally minimum when compared with PARAFAC algorithm because of the most elevated calculation errors of $RMSE_{PN}$ and $RMSE_{TN}$ as appeared in Figs. 7 and 8, separately. At the point when $SNR_{INPUT} = 20\ dB$, the SNR_{OUTPUT} created by Combined algorithm of Multidimensional Wavelet Packet Transform with Multiway Wiener Filter is just improved barely contrasted with the SNR_{INPUT}. Then again, when $SNR_{INPUT} = 40\ dB$. Combined algorithm of Multidimensional Wavelet Packet Transform with Multiway Wiener Filter develops the signal to noise ratio fundamentally. Yet, due to expand the emphases is expanded, the output of the signal to noise ratio is not steady. The conventional algorithm Multiple Linear Regression has better performance at output of signal to noise ratio in 20 dB, at the same time its performance is worst at 40 dB contrasted with Multidimensional Wavelet Packet Transform with Multiway Wiener Filter algorithm and proposed PARAFAC algorithm.

This pattern turns out to be more terrible as the SNR_{OUTPUT} of Multiple Linear Regression has minimum as compared to SNR_{INPUT}. The output graphs between output signal to noise at input signal to noise ratio 20 dB as well as 40 dB are shown in

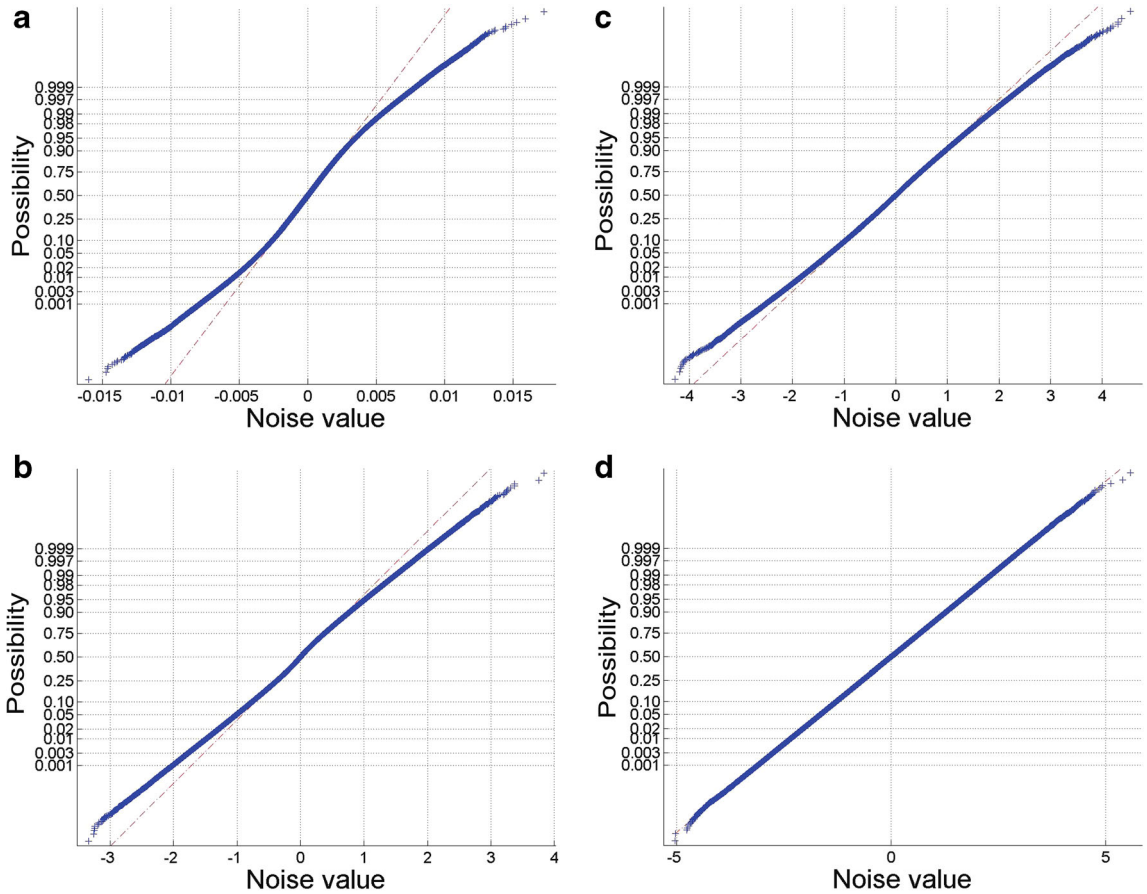

Fig. 11 **a** Possibility graph with noise at 40 dB (Pre-brighterning). **b** Possibility graph with noise at 40 dB (Using MLR). **c** Possibility graph with noise at 40 dB (Using MWPT-MWF). **d** Possibility graph with noise at 40 dB (Using PARAFAC)

Fig. 13a and b respectively. The Fig. 14 represents about the output of signal to noise ratio of every strategy. It demonstrates that conventional algorithm Multiple Linear Regression has improved better signal to noise ratio between 20 to 30 dB, but the signal to noise ratio decreases between 35 to 40 dB. The Combined algorithm of Multidimensional Wavelet Packet Transform with Multiway Wiener Filter has far more terrible performance and it has just a peripheral development of the signal to noise ratio during 20 dB. At the same time it decreases the signal to noise ratio between 25 to 40 dB. Finally we could presume that the proposed PARAFAC algorithm is a best algorithm than other solid denoising strategy for removal of noise in different noise situations.

Conclusion

In this paper, we have proposed and developed a new denoising framework called PARAFAC rank decomposition method based on tensor filtering algorithm for minimizing the signal independent noise (TN) and signal dependent noise (PN) simultaneously. The existing denoising methods such as Multiple Linear Regression and Combined algorithm of Multidimensional Wavelet Packet Transform with Multiway Wiener Filter have been experimented for the comparative study. The experimental results of all these techniques are looked at on account of photon noise brightening and denoising. The photon noise brightening test and the denoising test are intended to evaluate the parameter estimation performance. The simulation results shows that the performance of the proposed denoising framework called PARAFAC approach based on tensor filtering algorithm is better than other conventional denoising approaches and it has more efficient for reducing signal dependent (PN) and signal independent noise (TN). Hence this novel denoising approach would be more beneficial for detection of skin allergy and also this algorithm will be very useful for detection of retinal exudates and diagnosis of diabetes mellitus and retinopathy disease in medical application.

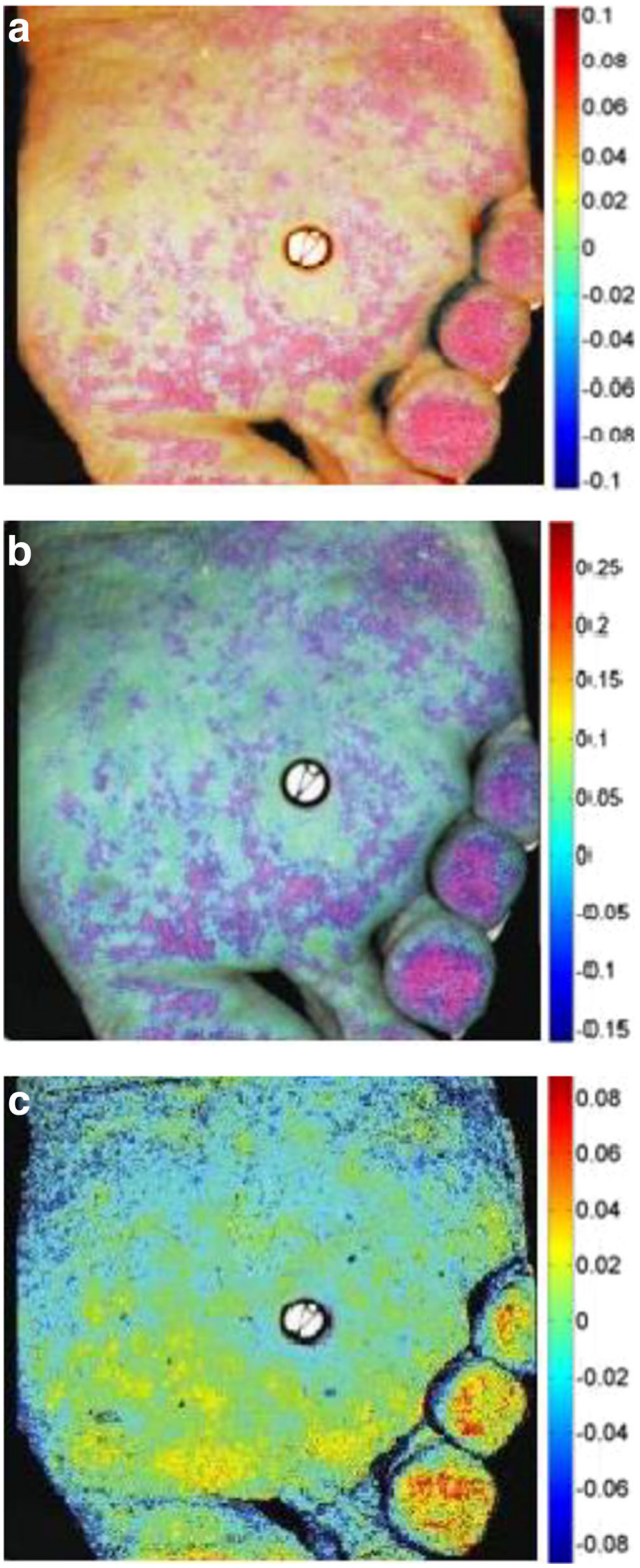

Fig. 12 **a** Noise removal using MLR, Band 10, $SNR_{INPUT} = 20$ dB. **b** Noise removal using MWPT-MWF, Band 10, $SNR_{INPUT} = 20$ dB. **c** Noise removal using PARAFAC, Band 10, $SNR_{INPUT} = 20$ dB

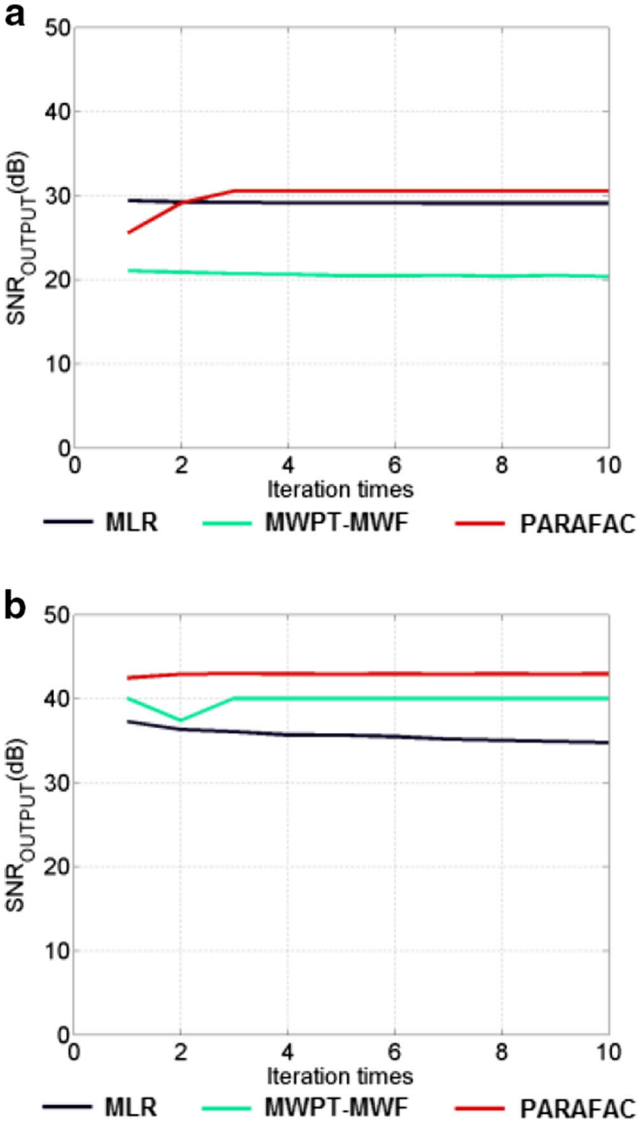

Fig. 13 **a** Output graph for SNR_{OUTPUT} vs various iteration period at SNR_{INPUT}: 20 dB. **b** Output graph for SNR_{OUTPUT} vs various iteration period at SNR_{INPUT}: 40 dB

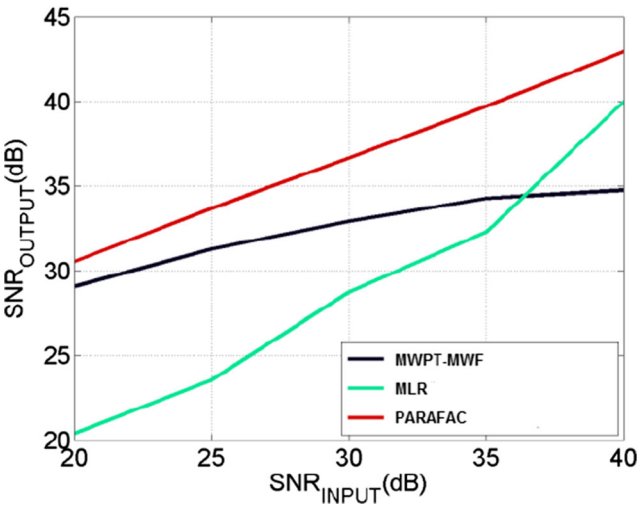

Fig. 14 Results comparison graph of SNR_{OUTPUT} vs SNR_{INPUT}

References

1. Bourennane, S., Fossati, C., and Lin, T., Noise Removal Based on Tensor Modelling for Hyperspectral Image Classification. Remote Sens. 10:1330, 2018.
2. Uss, M. L., Vozel, B., Lukin, V. V., and Chehdi, K., Local Signal-Dependent Noise Variance Estimation From Hyperspectral Textural Images. IEEE Journal of Selected Topics in Signal Processing 5(3): 469–486, 2011.
3. Alparone, L., Selva, M., Aiazzi, B., Baronti, S., Butera, F., and Chiarantini, L., Signal-dependent noise modelling and estimation of new-generation imaging spectrometers. In 2009 First Workshop on Hyperspectral Image and Signal Processing: Evolution in Remote Sensing, Grenoble, pp. 1–4, 2009.
4. Liu, X., Bourennane, S., and Fossati, C., Denoising of Hyperspectral Images Using the PARAFAC Model and Statistical Performance Analysis. IEEE Trans. Geosci. Remote Sens. 50(10): 3717–3724, 2012.
5. Gao, L., Yao, D., Li, Q., Zhuang, L., Zhang, B., and Bioucas-Dias, J. M., A New Low-Rank Representation based hyperspectral image denoising method for mineral mapping. Remote Sens. 9:1145, 2017.
6. Fan, Y. R., Huang, T. Z., Zhao, X. L., Deng, L. J., and Fan, S., Multispectral Image Denoising via Nonlocal Multitask Sparse Learning. Remote Sens. 10:116, 2018.
7. Atkinson, I., Kamalabadi, F., Mohan, S., and Jones, D. L., Wavelet-based 2-D multichannel signal estimation. In Proceedings International Conference on Image Processing (Cat. No.03CH37429), Barcelona, pp. 14–17, 2003.
8. Pizurica, A., and Philips, W., Estimating the probability of the presence of a signal of interest in multiresolution single- and multiband image denoising. IEEE Trans. Image Process. 15(3):654–665, 2006.
9. Letexier, D., and Bourennane, S., Noise Removal From Hyperspectral Images by Multidimensional Filtering. IEEE Trans. Geosci. Remote Sens. 46(7):2061–2069, 2008.
10. Renard, N., and Bourennane, S., Improvement of Target Detection Methods by Multiway Filtering. IEEE Trans. Geosci. Remote Sens. 46(8):2407–2417, 2008.
11. Aiazzi, B., Alparone, L., Barducci, A., Baronti, S., Marcoinni, P., Pippi, I., and Selva, M., Noise modelling and estimation of hyperspectral data from airborne imaging spectrometers. Ann. Geophys. 49(1):1–9, 2006.
12. Gao, L., Zhang, B., Zhang, X., Zhang, W., and Tong, Q., A New Operational Method for Estimating Noise in Hyperspectral Images. IEEE Geosci. Remote Sens. Lett. 5(1):83–87, 2008.
13. Aiazzi, B., Alparone, L., and S. Baronti, A robust method for parameter estimation of signal-dependent noise models in digital images. Proceedings of 13th International Conference on Digital Signal Processing, Santorini, vol.2, pp. 601–604, 1997.
14. Aiazzi, B., Alparone, L., Baronti, S., and Garzelli, A., Coherence estimation from multilook incoherent SAR imagery. IEEE Trans. Geosci. Remote Sens. 41(11):2531–2539, 2003.
15. Argenti, F., Torricelli, G., and Alparone, L., MMSE filtering of generalised signal-dependent noise in spatial and shift-invariant wavelet domains. Signal Process. 86(8):2056–2066, 2006.
16. Cheng, G., Li, Z., Han, J., Yao, X., and Guo, L., Exploring Hierarchical Convolutional Features for Hyperspectral Image Classification. IEEE Trans. Geosci. Remote Sens. 56(11):6712–6722, 2018.
17. Roger, R. E., Principal components transform with simple, automatic noise adjustment. Int. J. Remote Sens. 17(14):2719–2727, 1996.
18. Archibald, R., and Fann, G., Feature Selection and Classification of Hyperspectral Images With Support Vector Machines. IEEE Geosci. Remote Sens. Lett. 4(4):674–677, 2007.
19. Mallat, S. G., A theory for multiresolution signal decomposition: the wavelet representation. IEEE Trans. Pattern Anal. Mach. Intell. 11(7):674–693, 1989.
20. Muti, D., and Bourennane, S., Multidimensional filtering based on a tensor approach. Signal Process. 85(12):2338–2353, 2005.
21. Lin, T., and Bourennane, S., Hyperspectral Image Processing by Jointly Filtering Wavelet Component Tensor. IEEE Trans. Geosci. Remote Sens. 51(6):3529–3541, 2013.
22. Demirkesen, C., and Uğur, M. L., Estimation of noise model parameters for images taken by a full-frame hyperspectral camera. Image and Signal Processing for Remote Sensing XXI, 2015.
23. Bourennane, S., and Fossati, C., Dimensionality reduction and coloured noise removal from hyperspectral images. Remote Sensing Letters, 2015.
24. Bro, R., PARAFAC: Tutorial and applications. Chemom. Intell. Lab. Syst., 1997.

Publisher's Note Springer Nature remains neutral with regard to jurisdictional claims in published maps and institutional affiliations.